疫学情報　2020 年 3 月 19 日分
https://www.tuat.ac.jp/outline/disclosure/pressrelease/2019/20200313_01.html

2020 年 3 月 13 日　国立大学法人 東京農工大学
国立大学法人東京農工大学農学部附属国際家畜感染症防疫研究教育センター

新型コロナウィルス『COVID-19』検査の完全な自動化が可能に
～検査の負担軽減、信頼性向上、迅速化へ～

国立大学法人東京農工大学農学部附属国際家畜感染症防疫研究教育センターの水谷哲也教授および同大学院工学研究院生命機能科学部門の養王田正文教授は、新型コロナウイルス検出自動化に関する自動化技術の開発を行い、千葉県衛生研究所と共同で、サンプルから PCR 検査による判定までの全自動化に成功しました。

研究背景　：

今般、新型コロナウイルス『COVID-19』の蔓延が世界各地で重篤な健康被害を及ぼし、経済的影響も大きく取り上げられています。治療が困難なウイルス伝染や拡散を防ぐためには、PCR 検査による診断と接触の最小限化が不可欠であり、水際検査システムを確立する必要があります。

東京農工大学は、遺伝子解析の自動化技術開発を、千葉県の企業であるプレシジョン・システム・サイエンス株式会社（PSS 社）と共同で行ない、2020 年 3 月 10 日付けで以下の研究成果を発表しました。https://www.tuat.ac.jp/outline/disclosure/pressrelease/2019/20200310_01.html
この度、その成果として開発された全自動 PCR 装置「geneLEAD システム」が、新型コロナウイルス検出に有効であると考え、東京農工大学と千葉県衛生研究所の共同研究チームで、実サンプルを用いて検証した結果、その有効性を実証することに成功しました。

研究成果　：

この全自動 PCR 装置「geneLEAD システム」を用いることで、鼻咽頭拭い液や喀痰から PCR による判定までの完全な自動化が可能となりました。

分析時間は 2 時間 10 分であり、分析時間の短縮は限定的です。しかしながら、全自動であることから、検査者の負担を大幅に減らすことが可能となります。また、同時に、Human Error を低減することで、解析結果の信頼性の向上も期待できます。さらに、小型の装置であることから、病院などに設置することで、感染が疑われる患者の迅速検査への利用が期待されます。

今後の展開　：

今後は、東京農工大学、千葉県衛生研究所、PSS 社において、新型コロナウイルス『COVID-19』の検査への活用を検討し、実際の検査現場での分析に活用できるよう、準備を進めていく予定です。
https://www.tuat.ac.jp/documents/tuat/outline/disclosure/pressrelease/2019/20200313_01.pdf

https://www.nejm.org/doi/10.1056/NEJMc2004973
Aerosol and Surface Stability of SARS-CoV-2 as Compared with SARS-CoV-1

A novel human coronavirus that is now named severe acute respiratory syndrome coronavirus 2 (SARS-CoV-2) (formerly called HCoV-19) emerged in Wuhan, China, in late 2019 and is now causing a pandemic.[1] We analyzed the aerosol and surface stability of SARS-CoV-2 and compared it with SARS-CoV-1, the most closely related human coronavirus.[2]

We evaluated the stability of SARS-CoV-2 and SARS-CoV-1 in aerosols and on various surfaces and estimated their decay rates using a Bayesian regression model (see the Methods section in the Supplementary Appendix. opens in new tab, available with the full text of this letter at NEJM.org). SARS-CoV-2 nCoV-WA1-2020 (MN985325.1) and SARS-CoV-1 Tor2 (AY274119.3) were the strains used. Aerosols (<5 μm) containing SARS-CoV-2 ($10^{5.25}$ 50% tissue-culture infectious dose [$TCID_{50}$] per milliliter) or SARS-CoV-1 ($10^{6.75-7.00}$ $TCID_{50}$ per milliliter) were generated with the use of a three-jet Collison nebulizer and fed into a Goldberg drum to create an aerosolized environment. The inoculum resulted in cycle-threshold values between 20 and 22, similar to those observed in samples obtained from the upper and lower respiratory tract in humans.

Our data consisted of 10 experimental conditions involving two viruses (SARS-CoV-2 and SARS-CoV-1) in five environmental conditions (aerosols, plastic, stainless steel, copper, and cardboard). All experimental measurements are reported as means across three replicates.

Figure 1.

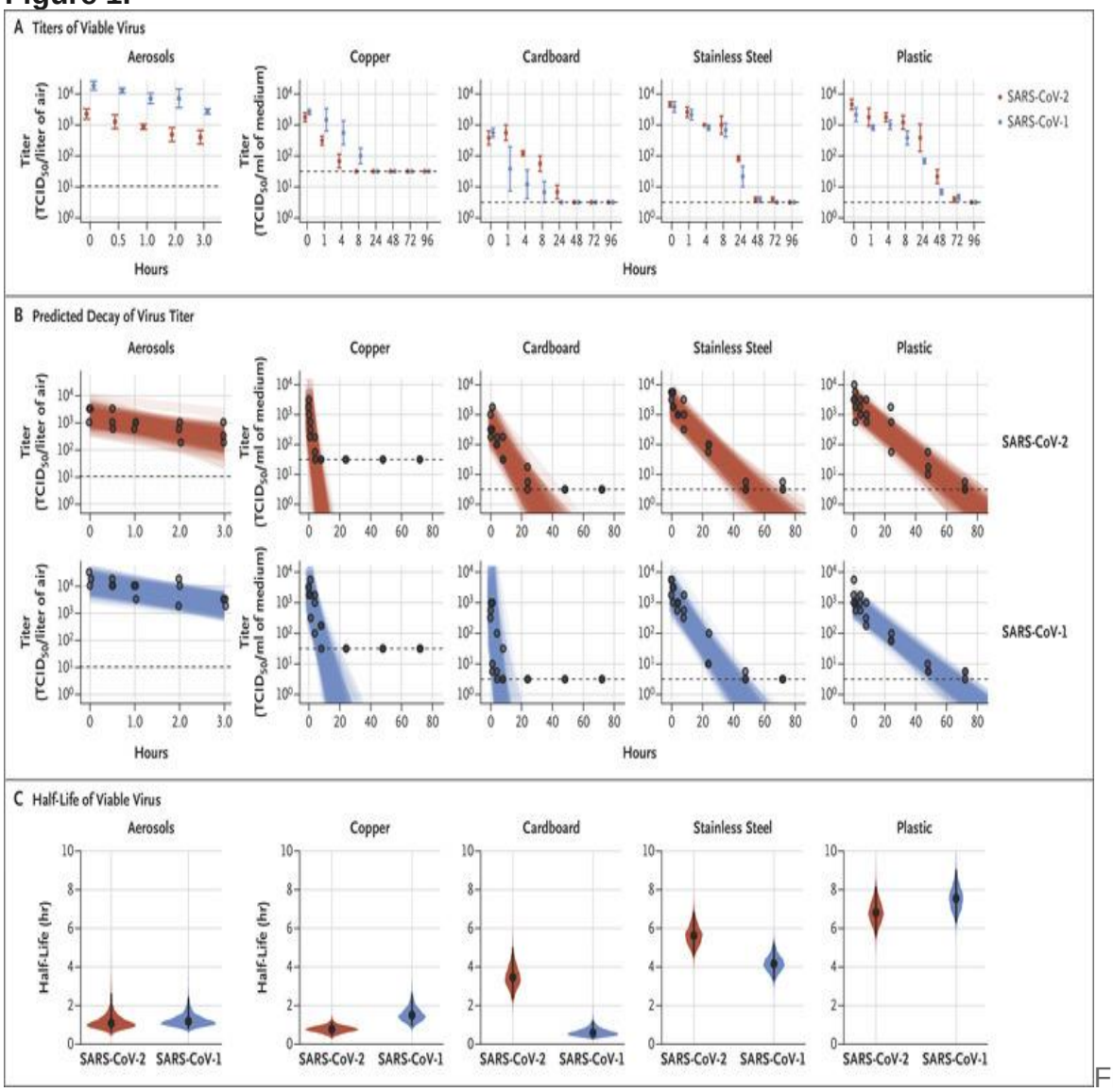

Figure 1. Viability of SARS-CoV-1 and SARS-CoV-2 in Aerosols and on Various Surfaces.

As shown in Panel A, the titer of aerosolized viable virus is expressed in 50% tissue-culture infectious dose ($TCID_{50}$) per liter of air. Viruses were applied to copper, cardboard, stainless steel, and plastic maintained at 21 to 23°C and 40% relative humidity over 7 days. The titer of viable virus is expressed as $TCID_{50}$ per milliliter of collection medium. All samples were quantified by end-point titration on Vero E6 cells. Plots show the means and standard errors (bars) across three replicates. As shown in Panel B, regression plots indicate the predicted decay of virus titer over time; the titer is plotted on a logarithmic scale. Points show measured titers and are slightly jittered (i.e., they show small rapid variations in the amplitude or timing of a waveform arising from fluctuations) along the time axis to avoid over plotting. Lines are random draws from

the joint posterior distribution of the exponential decay rate (negative of the slope) and intercept (initial virus titer) to show the range of possible decay patterns for each experimental condition. There were 150 lines per panel, including 50 lines from each plotted replicate. As shown in Panel C, violin plots indicate posterior distribution for the half-life of viable virus based on the estimated exponential decay rates of the virus titer. The dots indicate the posterior median estimates, and the black lines indicate a 95% credible interval. Experimental conditions are ordered according to the posterior median half-life of SARS-CoV-2. The dashed lines indicate the limit of detection, which was $3.33\times10^{0.5}$ $TCID_{50}$ per liter of air for aerosols, $10^{0.5}$ $TCID_{50}$ per milliliter of medium for plastic, steel, and cardboard, and $10^{1.5}$ $TCID_{50}$ per milliliter of medium for copper.

SARS-CoV-2 remained viable in aerosols throughout the duration of our experiment (3 hours), with a reduction in infectious titer from $10^{3.5}$ to $10^{2.7}$ $TCID_{50}$ per liter of air. This reduction was similar to that observed with SARS-CoV-1, from $10^{4.3}$ to $10^{3.5}$ $TCID_{50}$ per milliliter (Figure 1A).

SARS-CoV-2 was more stable on plastic and stainless steel than on copper and cardboard, and viable virus was detected up to 72 hours after application to these surfaces (Figure 1A), although the virus titer was greatly reduced (from $10^{3.7}$ to $10^{0.6}$ $TCID_{50}$ per milliliter of medium after 72 hours on plastic and from $10^{3.7}$ to $10^{0.6}$ $TCID_{50}$ per milliliter after 48 hours on stainless steel). The stability kinetics of SARS-CoV-1 were similar (from $10^{3.4}$ to $10^{0.7}$ $TCID_{50}$ per milliliter after 72 hours on plastic and from $10^{3.6}$ to $10^{0.6}$ $TCID_{50}$ per milliliter after 48 hours on stainless steel). On copper, no viable SARS-CoV-2 was measured after 4 hours and no viable SARS-CoV-1 was measured after 8 hours. On cardboard, no viable SARS-CoV-2 was measured after 24 hours and no viable SARS-CoV-1 was measured after 8 hours (Figure 1A).
Both viruses had an exponential decay in virus titer across all experimental conditions, as indicated by a linear decrease in the $\log_{10}TCID_{50}$ per liter of air or milliliter of medium over time (Figure 1B). The half-lives of SARS-CoV-2 and SARS-CoV-1 were similar in aerosols, with median estimates of approximately 1.1 to 1.2 hours and 95% credible intervals of 0.64 to 2.64 for SARS-CoV-2 and 0.78 to 2.43 for SARS-CoV-1 (Figure 1C, and Table S1 in the Supplementary Appendix. opens in new tab). The half-lives of the two viruses were also similar on copper. On cardboard, the half-life of SARS-CoV-2 was longer than that of SARS-CoV-1. The longest viability of both viruses was on stainless steel and plastic; the estimated median half-life of SARS-CoV-2 was approximately 5.6 hours on stainless steel and 6.8 hours on plastic (Figure 1C). Estimated differences in the half-lives of the two viruses were small except for those on cardboard (Figure 1C). Individual replicate data were noticeably “noisier” (i.e., there was more variation in the experiment, resulting in a larger standard error) for cardboard than for other surfaces (Fig. S1 through S5), so we advise caution in interpreting this result.

We found that the stability of SARS-CoV-2 was similar to that of SARS-CoV-1 under the experimental circumstances tested. This indicates that differences in the epidemiologic characteristics of these viruses probably arise from other factors, including high viral loads in the upper respiratory tract and the potential for persons infected with SARS-CoV-2 to shed and transmit the virus while asymptomatic.[3,4] Our results indicate that aerosol and fomite transmission of SARS-CoV-2 is plausible, since the virus can remain viable and infectious in aerosols for hours and on surfaces up to days (depending on the inoculum shed). These findings echo those with SARS-CoV-1, in which these forms of transmission were associated with nosocomial spread and super-spreading events,[5] and they provide information for pandemic mitigation efforts.

Neeltje van Doremalen, Ph.D.
Trenton Bushmaker, B.Sc.
National Institute of Allergy and Infectious Diseases, Hamilton, MT

Dylan H. Morris, M.Phil.
Princeton University, Princeton, NJ

Myndi G. Holbrook, B.Sc.
National Institute of Allergy and Infectious Diseases, Hamilton, MT

Amandine Gamble, Ph.D.
University of California, Los Angeles, Los Angeles, CA

Brandi N. Williamson, M.P.H.
National Institute of Allergy and Infectious Diseases, Hamilton, MT

Azaibi Tamin, Ph.D.
Jennifer L. Harcourt, Ph.D.
Natalie J. Thornburg, Ph.D.
Susan I. Gerber, M.D.
Centers for Disease Control and Prevention, Atlanta, GA

James O. Lloyd-Smith, Ph.D.
University of California, Los Angeles, Los Angeles, CA, Bethesda, MD

Emmie de Wit, Ph.D.
Vincent J. Munster, Ph.D.
National Institute of Allergy and Infectious Diseases, Hamilton, MT
vincent.munster@nih.gov

Supported by the Intramural Research Program of the National Institute of Allergy and Infectious Diseases, National Institutes of Health, and by contracts from the Defense Advanced Research

Projects Agency (DARPA PREEMPT No. D18AC00031, to Drs. Lloyd-Smith and Gamble), from the National Science Foundation (DEB-1557022, to Dr. Lloyd-Smith), and from the Strategic Environmental Research and Development Program of the Department of Defense (SERDP, RC-2635, to Dr. Lloyd-Smith).
Disclosure forms. opens in new tab provided by the authors are available with the full text of this letter at NEJM.org.

The findings and conclusions in this letter are those of the authors and do not necessarily represent the official position of the Centers for Disease Control and Prevention (CDC). Names of specific vendors, manufacturers, or products are included for public health and informational purposes; inclusion does not imply endorsement of the vendors, manufacturers, or products by the CDC or the Department of Health and Human Services.